

Greenery as a mitigation strategy to urban heat and air pollution: a comparative simulation-based study in a densely built environment.

Abstract

The urban heat island and the urban air pollution concentration are two major climate-change-related phenomena affecting the built environment worldwide. This paper aims to verify the potential effect of different mitigation measures through a simulation study. In detail the present study focuses on the analysis of the environmental impacts of urban vegetation, such as green facades, vertical greenery, and green pavements. After an extensive screening of the literature review, an investigation of the impact of the most common built environment design variables in a defined case study led to the definition of a typical urban canyon was tested. The results show that the presence of trees in a street canyon could reduce the air temperature peaks by 5-10 °C, while the high-level vegetation canopies can lead to a deterioration in air quality with a PM concentration increasing by 1.2-1.5%. Instead, using low-level green infrastructure improves the air quality conditions on the sidewalk, reducing the NOx in the range of 10-20%. The analyzed high-level greenery generated an air temperature reduction effect on a street level ranging from 8 to 12°C. The present work contributes to clarifying the potential mitigation effect of green infrastructure in a densely built environment, where the risk of increasing temperatures and air pollutants is foreseen to be more intense in the coming years.

Keywords: Urban Heat Island, Air Pollution, Mitigation Strategies, Built Environment, Resilience

1. Introduction

Greenhouse gas emissions are progressively less driven by industrial activities and instead mainly originate from energy services required for providing suitable indoor environments (e.g., heating and cooling, lighting, appliances) and mobility [1]. In addition, cities are becoming greyer: they are made of dense building materials, absorbing energy from the sun; fewer trees to provide shade and cooling effect; and fewer green areas to cool by evapotranspiration and absorb air pollutants. Thus, cities are becoming more frequently prone to suffer intense Urban Heat Island (UHI) and Air Pollution (AP), especially within dense Built Environments (BE).

In addition, cities and dense urban areas are now more densely populated. Therefore, more people would be exposed to UHI and related risks. In fact, the United Nations estimated that in 2018, 55% of the world's population lived in urban areas, and in the next two decades, it will reach 66% [2]. In particular, cities' common characteristics enhance UHI and AP related to Slow Onset Disaster (SLOD) risks; that is: low albedo materials, human gatherings, increased use of air conditioners, reduced green areas, urban canopy, blocked wind flow and pollutant emission [3]. In order to contrast such conditions, existing literature has reported that the presence of vegetation plays a key role in improving air quality and enhancing the microclimate of the open space [4].

Consequently, this research work aims to study natural-based solutions, testing and quantifying the potential impact that selected green mitigation strategies (MS) (i.e., hedges, trees, and green facades) can have at a large scale and their effectiveness in different contexts based on the comparison of PET (Physiological Equivalent temperature), NOx concentrations and PM concentrations as performance indicators. The large-scale impact is extrapolated from the results of different computer-aided simulation tools on the study case's simplified urban canyon archetype. These simulations were also employed to perform sensitivity analysis on influencing parameters to explore multiple configurations and effects. In addition, the presented work can be embraced as a protocol for designers to demonstrate the relevance of some design decisions toward a more salutogenic urban design. Finally, in contrast with some of the previous works on UHI, the analysis is focused on reducing the stress on pedestrians during daylight hours instead of studying nocturnal UHI.

1.1 Overview of UHI and AP mitigation strategies

Evidence on the UHI effect and AP have been documented in cities worldwide [5]. As mentioned before, cities are more likely to suffer these phenomena, and certain portions of the city are more prone to increase the intensity of UHI and AP [3].

49 Although several studies have researched the causes of UHI and AP and the possibilities to reduce them, most have
50 focused on the relevance of urban morphology and materials to environmental conditions [6][7]. The geometry of the
51 canyon influences the urban energy balance in various ways. For example, it increases/decreases the surface exposed to
52 the exchange processes (allows/blocks solar radiation influx), determines the level of interaction between the surfaces
53 that compose the BE, limits/augments the ability to disperse the long-wave infrared radiation, and limits/enhances air
54 turbulence. Regarding canyon morphology, the parameters proven most influential on temperature and radiation
55 exchanges are canyon orientation, aspect ratio (H/W), and sky view factors [8]. For example, according to [9], the
56 building disposition directly impacts temperature levels: in narrow street canyons, the air temperature increase by 2-4°C.
57 In fact, long and narrow street canyons are characterized by poor ventilation (i.e., low wind velocity), which in addition
58 contributes to the accumulation of air pollution. At street intersections, buildings should be recessed, and open plazas or
59 green spaces should be created to stimulate the diversion and distribution of wind flows to different directions; hence,
60 avoiding the formation of vortex zones that hamper the dispersion of air pollutants. Nevertheless, these are not very likely
61 to change in a privately owned area of a dense urban space.

62 Instead, it is more likely to profit from the properties of cool surface materials/typologies within urban areas to greatly
63 contribute to tackling the UHI. For instance, the extensive use of high-albedo or highly reflective materials has been
64 advocated to mitigate the urban heat island, especially in warm-climate cities [10]. These properties determine how the
65 sun's energy is reflected, emitted, and absorbed [1]. By increasing the reflectivity of the building materials, there is a
66 reduction of daytime surface temperature, mainly during the summer season. In fact, it has been proven that under the
67 same peak solar conditions, the surface temperature for a black material is about 50°C higher than the air temperature.
68 In comparison, for a white material, the surface temperature is only 10°C higher [15]. Specific building surface types,
69 such as cool roofs, reduce, in the long-term, the temperature of the urban environment; they are characterized by materials
70 with high albedo coefficient and/or evapotranspiration (e.g., water pond), allowing materials to stay up to 28–33°C cooler
71 than conventional rooftops during peak summer [15]. Also, the high reflectivity of building walls tends to decrease the
72 canopy air temperature [15].

73 However, some constraints should be considered for the strategies: restricting the maximum pavement albedo to
74 avoid potential glare effects on drivers and pedestrians and increased reflected solar radiation directly towards pedestrians
75 resulting in higher thermal stress (thus, lower outdoor thermal comfort).

76 On the other hand, it is possible to act on the building envelope by using photocatalytic materials to manage AP.
77 These types of interventions allow air purification by contrasting the concentration of particles through the degradation
78 of nitrogen oxides. But these materials must be constantly maintained to avoid diminishing their air purification capacity
79 due to saturation.

80 In contrast, green strategies have been documented to contribute significantly to both phenomena, without intrusive
81 interventions on the built fabric and with rather a positive impact on the building performance and pedestrians' comfort
82 [15].

83 *1.2 Strategies targeting UHI and AP with the presence of high and low-level greenery*

84 The use of high and low-level vegetation (e.g., trees and hedges) is also widely recognized, in general, as a promising
85 strategy for mitigating UHI and AP [14]. It can regulate and lower surface and air temperatures through the
86 evapotranspiration process and by providing shading, which directly reduces the building's consumption during the
87 summer season, a higher outdoor thermal sensation, and a lower heat stroke risk [15]. Moreover, the most suitable tree
88 and plant can be chosen according to their size (i.e., canopy dimensions), seasonality (evergreen/seasonal), and pollutant
89 absorption characteristics [17].

90 It is widely agreed that green areas integrated into the BE can improve air quality conditions by acting as natural
91 filters of air pollutants [18]. Still, within street canyons, high-level vegetation canopies (trees) have led to a deterioration
92 in air quality, while low-level green infrastructure (hedges) improved air quality conditions. The use of shrubs or hedges
93 with heights lower than 2 m should be encouraged to improve roadside air quality, and large, dense trees should be
94 avoided around roads with heavy traffic [9]. The greenery position is also important; roadside trees and hedges reduce
95 the heat perception in highly polluted areas [19].

96 Also, it has been demonstrated that leaves can deposit and capture particulates on their surface [20], and plants'
97 presence increases the turbulence of the air flows, which favors the dispersion of the pollutants particles [21]. Therefore,
98 green areas are highly recommended near highly trafficked zones or those likely exposed to sensitive demographic groups
99 (e.g., schools and hospitals) [22].

100
101 Regarding the materials used in the BE, high albedo, high thermal emissivity, and low heat capacity play a key role
102 in UHI mitigation [11]. For instance, vegetative facades can also reduce up to 7.7°C the surface temperature peaks of the

103 building facades through evapotranspiration and shading in summer [24] and increase the thermal insulation in winter.
104 The use of green roofs with limited vegetation (e.g., extensive green roofs with sedum herbs) can moderate the effect of
105 the urban heat island, especially during the day, reducing surface temperature up to 5°C [12] and on top city-wide ambient
106 temperature up to 10°C [15]. However, the extent of these MS depends on climate, plants' density foliage, and land
107 coverage intensity.

108 Nevertheless, UHI should also be tackled at ground level to directly improve the quality of the surroundings for
109 pedestrians. Increasing green areas (intended as heat sinks) can lower air and surface temperatures at the street level
110 during the day. Vegetative facades can be another solution, improving building energy performance while absorbing
111 pollutants. Moreover, when integrated with the built environment, large areas of greenery (e.g., urban forest) help
112 suppress dust particles, improving air quality around buildings and busy highways; and reducing inhabitants' respiratory
113 illness. Green roofs can also be used as effective air pollution abatement measures [25]. However, their ability to remove
114 pollutants is normally lower compared to trees, vegetation barriers, and green walls, given their low surface roughness
115 and distance away from pollutant sources [26]. Nevertheless, green roof technologies require less walkable space than
116 trees and green belts and can be adapted to arrange part of building surfaces and structures such as bridges, flyovers,
117 retaining walls, and noise barriers.

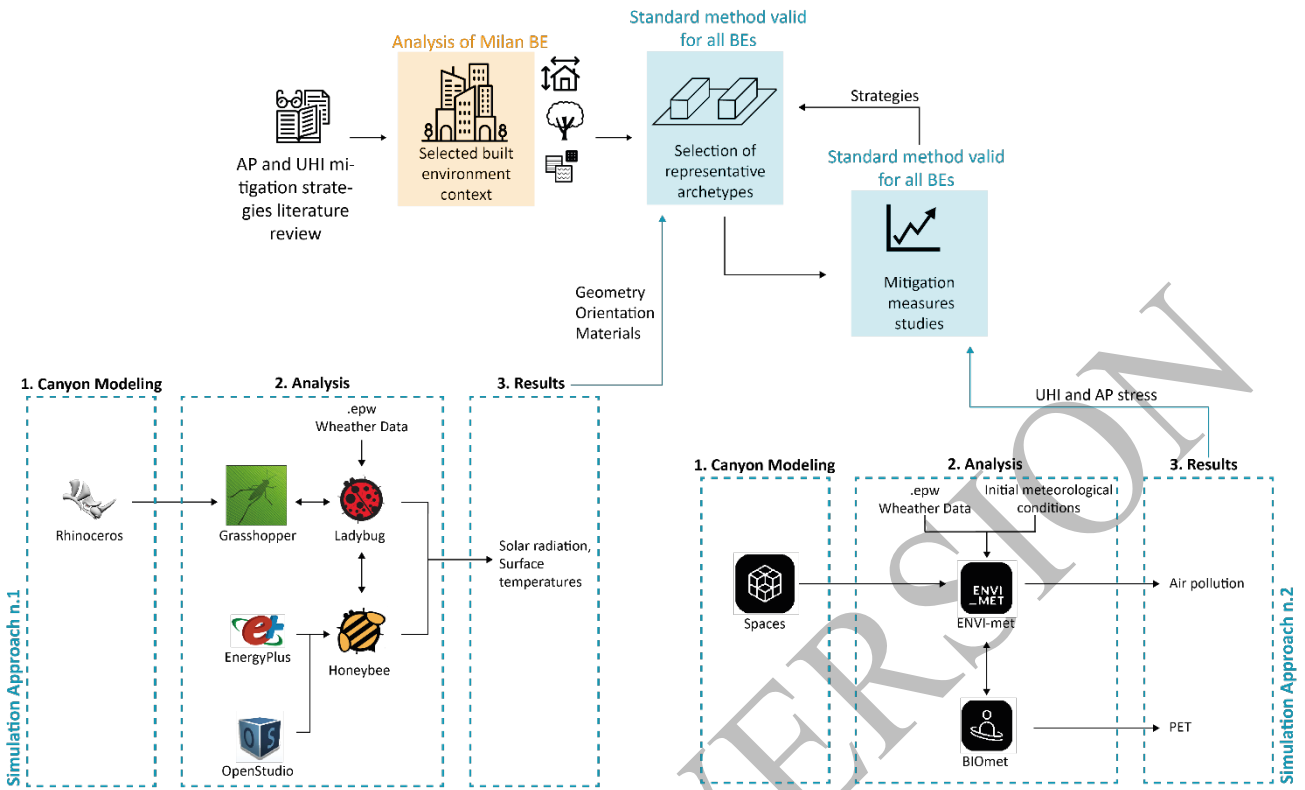
118 Although direct reductions of traffic emissions have been enforced, passive pollutant control measures are considered
119 suitable for remedy. Areas with limited natural ventilation in the street canyons enhance the accumulation of air pollutants
120 at the footpath level, augmenting exposure for pedestrians. In this context, solid and porous vegetative structures
121 immersed in urban street canyons (e.g., low boundary walls, shrubs, hedges), which affect less wind flow and pollutants
122 dispersion, should be preferred.

123 Most of the screened literature and previous works on greenery MS have concentrated on analyzing large portions
124 of the urban built environment or open areas, thus, reducing the possibility of extrapolating the analysis to the rest of the
125 urban space or other contexts. Moreover, most strategies have been tested singularly by tackling one aspect only (UHI
126 or AP), without combining different greenery MS, specifically trees combined with green facades. Therefore, this work
127 has concentrated on studying in parallel the UHI and AP effect of singular and combined greenery MS on a basic
128 typological urban unit.

129 **2. Methods**

130 In order to measure the effect of selected MS, different tools have been integrated into a structured workflow because
131 of their capabilities, the required computing time, and the large number of variables to consider. The simulation process
132 has been divided into two steps, and the whole procedure has been summarized in Figure 1. As described in §2.1, the
133 first part comprised a set of parametric simulations with Rhino and Ladybug Tools to construct and analyze different
134 urban unit archetypes considering the surface materials' dimension, orientation, and albedo. This preliminary study led
135 to finding and establishing the most critical and representative archetype configuration, heat-wise, characterized by
136 higher solar exposure and mean radiant temperature; as the tested parameters do not modify the air pollutant distribution,
137 and no wind direction was set at this stage. The second part encompassed a set of simulations for evaluating the
138 effectiveness of the green MS on the defined canyon archetype, all modeled with ENVI-met.

139



140

141

142

Figure 1. General description of the methodology proposed for detailed UHI and AP analysis within the BE.
 2.1 Canyon archetype and site-specific mitigation tests

143

144

145

146

147

148

149

150

This step is focused on narrowing the typical geometrical characteristics (i.e., H/W and orientation) and materials (albedo). In this respect, Rhinoceros and Grasshopper have been chosen to test different canyon configurations parametrically. Initially, the 3-dimensional geometry is constructed using Rhinoceros. Then, Grasshopper and Ladybug Tools are exploited to parametrically set the environmental conditions and compute the behavior of solar radiation and surface temperatures. Specifically, Ladybug has been used to perform and visualize detailed climate data analysis for supporting environmentally informed design. It has also been used to import standard EnergyPlus Weather files (.epw) into the Grasshopper environment. Instead, Honeybee (coupled with OpenStudio and EnergyPlus) was used to run and visualize solar radiation distribution simulations, to study surface temperatures of building facades and ground.

151

152

153

154

155

156

All the simulations have been carried out on canyons with buildings with heights equal to 25 m and different road widths ($H/W < 0.80$). The geometry has been selected as a representative representation of a typical suburban Italian city area characterized by buildings with floors ranging from 5 to 12. In order to avoid having a significant impact on the edge effect, a reduced analysis grid surface has been placed in the center of a 100 m-long canyon to speed up the simulation process and enable the study of all involved variables. The analysis grid is 10 m wide and has a sensor spacing of 2 m, which covers both sides of the canyon's building facades and the road width.

157

158

159

160

161

162

163

164

The simulations on the canyons were tested under the Milanese climate context on June 21st, selected as a representative summer day characterized by high solar radiation and elevated air temperatures. Different combinations of H/W ratios, albedo coefficients, and orientations have been tested, providing information on the incoming solar radiation and surface temperatures, useful to determine the most critical canyon configuration to try the MSs later. The relevant radiative properties of surface materials have been selected from the approximate values and ranges presented in BS 8206-2 [27] and by Salleh et al. (2014) [28]. The simulation settings for this preliminary study have been summarized in Table 1. A total of 13 simulations have been conducted and compared. The configuration that can guarantee lower solar exposure and lower surface temperature distribution has been selected for each simulation.

165

166

167

168

169

170

The tests have been planned to select a relevant canyon width before testing the canyon orientation and finishing radiative properties. The selection of the H/W ratio to study in depth is based on the criticality of the conditions found and their representativity. Likewise, the effect of the canyon orientation/azimuth has been evaluated by rotating the canyon 0° , 45° , 60° , 90° , 135° and 150° from the north, and a relevant orientation has been selected to further consolidate a canyon archetype. Finally, different façade finishing surface colors (i.e., white, grey, and black) have been allocated and compared to see their variance and select the most appropriate for the canyon archetype.

Grid properties				
Grid size dimension	x-nodes	100		
	y-nodes	150		
	z-nodes	50		
Size of grid cell in meter	dx	2 m		
	dy	2 m		
	dz	2 m		
Canyon Geometry				
Canyon length	100 m			
Building width	15 m			
Building height	25 m			
Canyon width	15 m / 20 m / 25 m / 30 m			
Weather data				
Climate file [.epw]	Milan (Linate Airport)			
Analysis period				
Solar radiation analysis	21 st June for 24 hours			
Surface temperatures analysis	21 st June from h14.00 to h16.00			
Canyon azimuth				
North orientation	0° / 45° / 60° / 90° / 135° / 150°			
Common color associated radiative properties				
Percentage of absorbed solar radiation	White	25 %		
	Grey	50 %		
	Black	90 %		
Surface Material associated properties				
	Asphalt	Ground	Plaster	Walling
Roughness	Elevated	Elevated	Low	Medium
Thickness [m]	0.5	2	0.025	0.13
Conductivity [W/mK]	0.75	0.32 - 4	0.6918	0.89
Density [kg/m ³]	2360	2050	1858	1920
Specific Heat [J/kgK]	960	800 - 1480	836	790
Thermal absorption coefficient [%]	90	70	50	50

Table 1. Energy model and simulation settings of the selected representative canyon following the described Approach 1 in Figure 1.

2.2 BE mitigation strategies tests

After selecting the typical canyon, the second part of the simulations study was carried out through the ENVI-met environment to analyze the potential effect of different MSs on the chosen geometry.

This software is a validated three-dimensional computational fluid dynamics (CFD) model tailored for parallel simulating urban atmospheric processes, such as pollutant dispersion and microclimate effect. The flow solver of this program is based upon the Reynolds averaged Navier-Stokes (RANS) equations and uses the E-ε model for turbulence effects. This software has been exploited in this work to obtain results on perceived temperatures and air pollution concentration distribution (i.e., PM and NO_x).

The geometrical model has been directly constructed on ENVI-met's GUI, and a grid of 100x150x50 cells, each of 2x2x5m, has been set for analysis. Within this area, the identified critical street canyon has been modeled. Buildings have been modeled following the most common construction characteristics of the Italian BE, selecting a moderately insulated wall and roof with a surface material with a medium albedo coefficient (albedo = 0.5). Then, only traffic has been added as a pollution source, which has been modeled as linear along the canyon, considering daily intensity variations. The heat stress is computed as Physiological Equivalent Temperature (PET) [29] for a representative pedestrian based on the representative building occupant described on ISO 8996 [30]. Different strategies are applied

189 and tested independently once the street canyon has been modeled with its materials and sources. For the MS based on
190 vegetation, one type of tree, hedge, and green wall have been selected with the characteristics summarized in Table 2.
191 Following the approach in §2.1, simulations were carried out on June 21st, but on only the warmest sunlit half of the day,
192 to avoid extensive simulation times and ensure both critical temperatures and pollution are present. The time window has
193 been selected for including the highest solar radiation intensity and the most polluted hours (during the evening). The
194 results obtained from these simulations have been later used to evaluate and compare the effectiveness of strategies to
195 provide guidelines for urban planners, aiming at mitigating the UHI and AP phenomena.

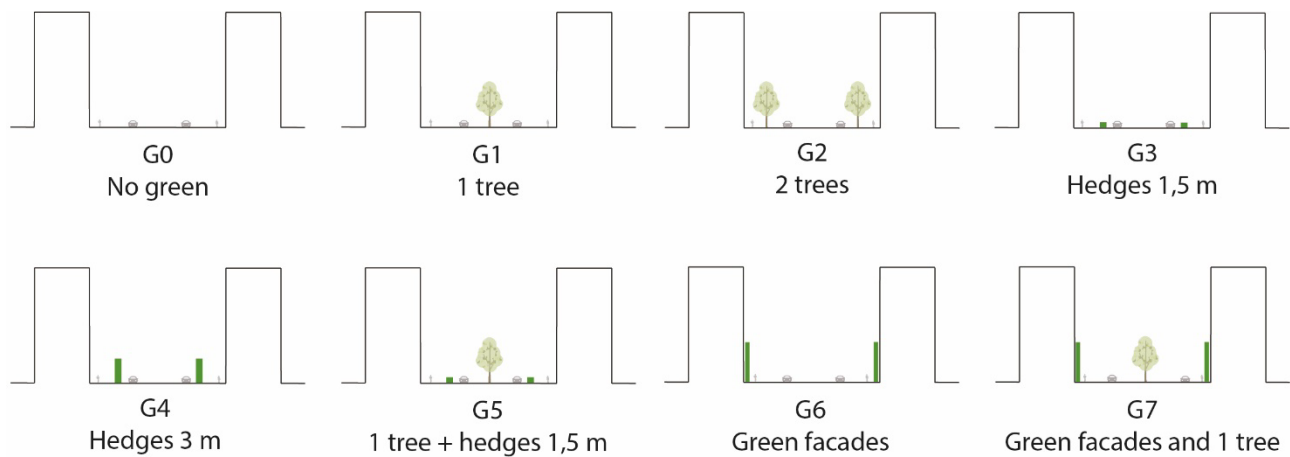
IN-PRESS VERSION

Grid properties			
Model dimension:	x-grids	100	
	y-grids	150	
	z-grids	50	
Size of grid cell in meter	dx	2 m	
	dy	2 m	
	dz	5 m	
Method of vertical grid generation	dz of lowest gridbox is split into 5 subcells		
Nr. of nesting grids	5		
Geometry			
Canyon length	100 m		
Building width	15 m		
Building height	25 m		
ENVI-met Weather data (initial conditions)			
Wind measured in 10 m height m/s	0.5		
Wind direction	NORTH		
Roughness length at measurement site	0.01		
Min and max temperature of atmosphere	14 – 30 °C		
Min and max relative humidity in 2m	50 - 75 %		
Buildings' materials			
Typology	Default wall – moderate insulation		
Thickness of layer:	0.01 plaster - 0.12 insulation - 0.18 concrete		
Possible usage	Wall or roof		
Roughness length	0.02		
Albedo	0.5		
Traffic			
Default height	0.15 m		
Source geometry	Line		
Daily traffic value veh/24h	8000 (Medium/High intensity)		
Number of lanes in the street segment	2		
LDV (light duty vehicles)	5%		
HDV (heavy duty vehicles)	2.5%		
MC (motorcycles)	0.5%		
Urban bus (public transport)	3%		
Coaches	1%		
Cars	88%		
	Loamy soil	Asphalt	Grey pavement
z0 roughness length	0.015	0.01	0.01
Albedo	0	0.2	0.5
Emissivity	0.98	0.9	0.9
Background pollutants concentration			
NO	10 µg/m ³		
NO ₂	90 µg/m ³		
Ozone	60 µg/m ³		
PM 10	40 µg/m ³		
PM 2.5	30 µg/m ³		

Trees characteristics	
Typology	Platanus x Acerifolia
Height	15 m
CO ₂ fixation type	C3 - Plant
Leaf type	Deciduous Leaves
Foliage shortwave albedo	0.18
Foliage shortwave transmittance	0.3
Leaf weight [g/m ²]	100
Isoprene capacity	12
Green Wall characteristics	
Typology	Green facade + mixed substrate
Wall height	5 m
Plant thickness	0.15 m
Albedo	0.2
Substrate thickness	0.15 m
LAI [m ² /m ²]	1.5
Leaf angle distribution	0.5
Emissivity of substrate	0.95
Water coefficient of substrate for plant	0.5
Air gap between substrate and wall	0.1
Hedge characteristics	
CO ₂ fixation type	C3
Leaf type	Deciduous
Albedo	0.2
Transmittance factor of leaf for shortwave radiation	0.3
Plant height	1.5 – 3 m
Root zone Depth	0.5
Leaf Area (LAD) Profile	2.5
Root Area (RAD) Profile	0.1
Season Profile	1
Average male human parameters	
Age of person	35
Gender	male
Weight	75 kg
Height	1.75 m
Surface area	1.91 m ²
Static Clothing Insulation (clo)	0.9
Total metabolic rate	86.21 W/m ²

Table 2. ENVI-met model and simulation settings, considering materials, geometry, traffic, vegetation, and specific simulation inputs.

Different greenery MS have been foreseen and grouped into 7 types (G1-G7) (Figure 2) which have been applied individually or combined. The results have been compared based on the absolute arithmetic difference of PET, NO_x, and PM concentrations between the current state and the cases with greening MS.



203

204

Figure 2 Representation of the seven tested greenery solutions for UHI and AP mitigation strategies.

205

206

207

As discussed in §1, vegetation can improve the UHI and air quality. The selected natural-based MS (Figure 2) comprises the use of single or multiple-row trees, hedges with different heights (1.5 m or 3 m) on the sidewalk, and green facades (5 m height).

208

3. Results

209

3.1 Selection and study of representative archetype: simulation results analysis

210

211

212

213

This section presents the results of simulation approach 1 (Figure 1) for selecting the typical BE archetype. Different H/W, orientations, and albedo coefficients were combined and tested (Table 1); regarding the width of the canyon, different dimensions were considered (while orientation and albedo remain fixed) given the assumption that in dense BE, it is common to have both large avenues and small secondary roads.

214

215

216

217

218

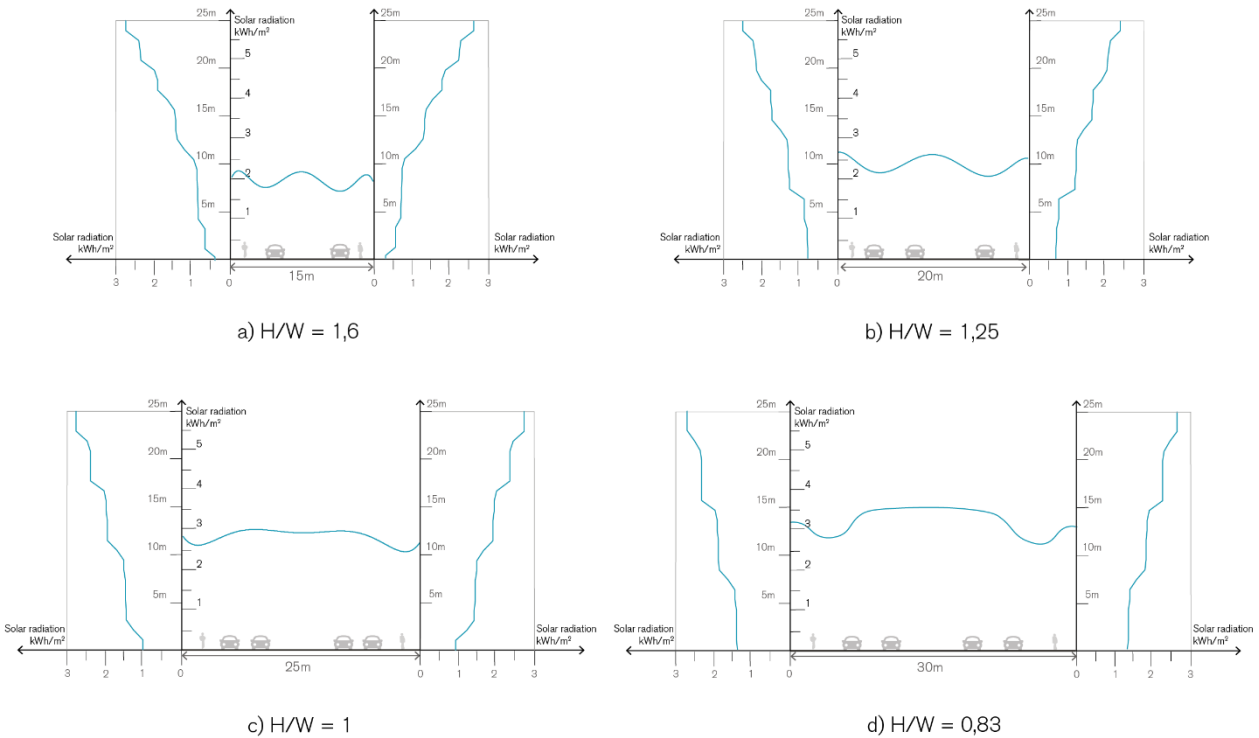
219

220

221

222

Simulations were conducted by analyzing the solar radiation intensity on different canyon configurations at 0° azimuth during the summer solstice's hottest hours (14:00 to 16:00) (June 21st). Figure 3 shows the estimated solar radiation distribution on outdoor surfaces for the different composed canyon geometries. The canyons with aspect ratios $H/W = 1$ and 0.83 resulted in the highest intensity of solar radiation during the investigated hours (solar horizontal distribution level approximately equal to 3 kWh/m^2). As reported in the following sections, the authors selected the case study with an aspect ratio H/W equal to 1 for the in-deep simulation study. The solar radiation on the vertical surface of the canyon is comparable with the widest configuration showing a similar mirrored shadow trend produced by the building facades. Thus, a geometry with two sidewalks, two carriageways for each direction, and additional space for trees in the center and/or on the sides has been chosen, considering that it is representative of most of the BE.



223

224

Figure 3. Solar radiation analysis on June 21st for different H/W urban canyons oriented at 0°.

225

226

Different canyon orientations have also been analyzed since the city's streets do not always follow a defined and regular orthogonal grid. From north, 0°, 45°, 60°, 90°, 135° and 150° have been tested as relevant street directions.

227

228

229

230

231

232

233

234

As shown in Figure 4, the incident solar radiation changes significantly for a canyon with the same geometry and different orientations. In a canyon-oriented north/south (Figure 4 a), the curves are symmetrical, indicating that, during the sun hours, both sides of the canyon are exposed equally. Rotating the geometry, as expected, one side of the canyon is more directly exposed to the sun with respect to the opposite side. Moving to East/West, the solar radiation becomes irregular, with the exposed side having 45% more solar radiation and the other side 66% less than the North/South orientation. The canyon rotated by 45° to the east (Figure 4 b) has been selected as a relevant archetype because it shows a good compromise among the different configurations with a reduced solar exposure mismatch (25%) between the different canyon sides.

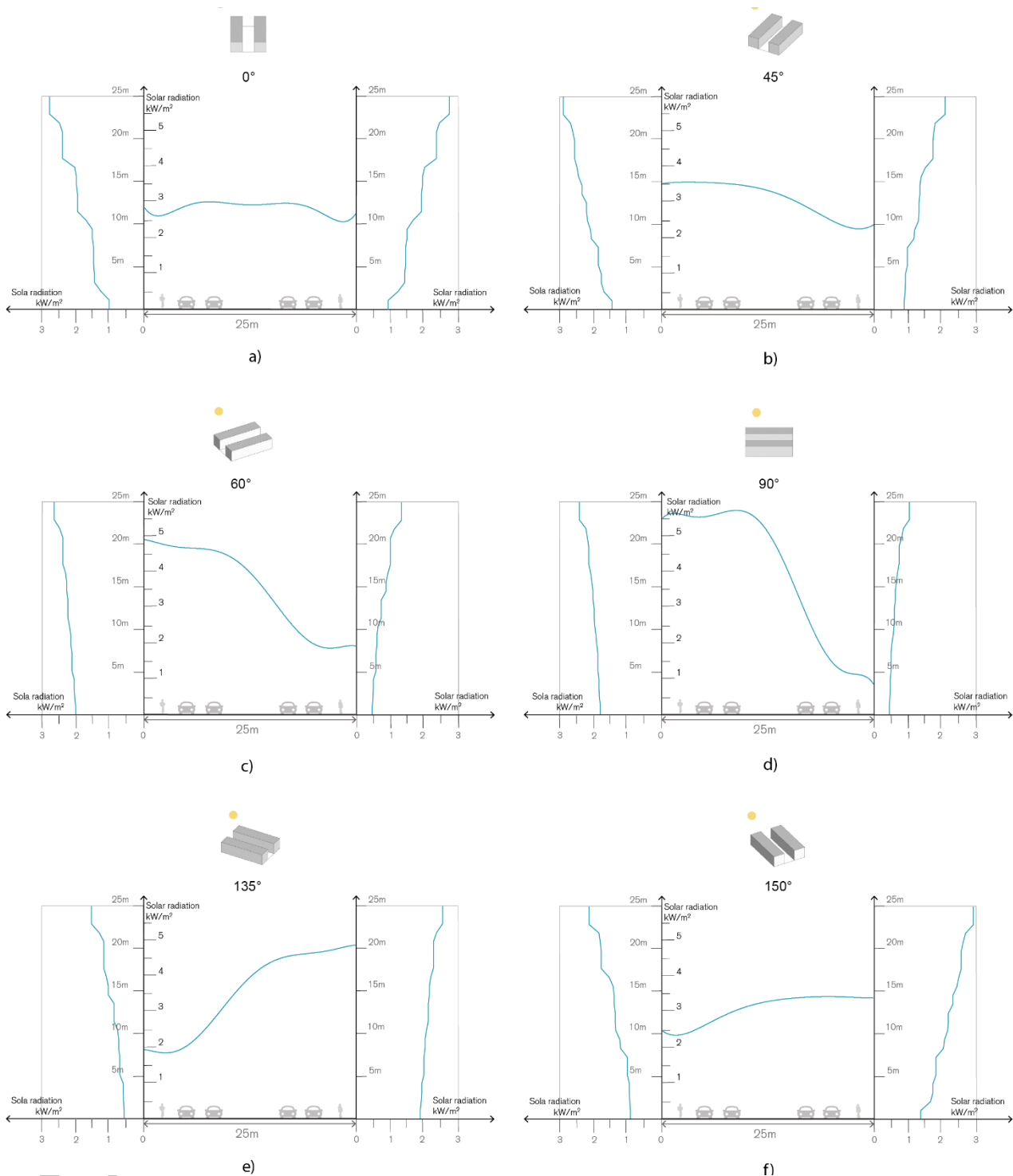


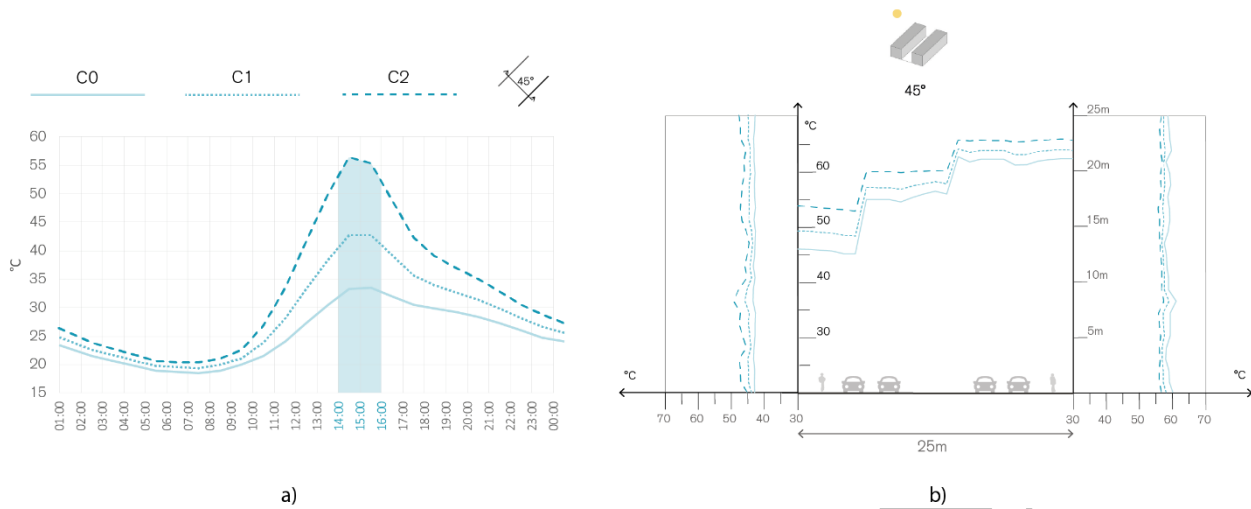
Figure 4. Solar radiation analysis (June 21st) for different orientations
 a) 0°; b) 45°; c) 60°; d) 90°; e) 135°; f) 150°.

235
 236
 237

238 After setting the geometry and orientation of the canyon, three different finishing colors, resulting in different albedo
 239 coefficients, have been analyzed: C0 - white ($\epsilon = 0.8$, $\rho = 0.85$), C1 - Grey ($\epsilon = 0.55$, $\rho = 0.94$) and C2 - Black ($\epsilon = 0.2$, ρ
 240 = 0.96). These represent the extremes and a balance option in terms of reflectivity and emissivity of the surfaces. The
 241 results have been summarized in Figure 5.

242 The simulations have been carried out from 13:00 to 20:00 on June 21st concerning the impact of the surface
 243 materials on temperatures level. Figure 5 b) shows the temperature level for all three selected façade colors applied to
 244 the canyon archetype. As expected, the maximum surface temperature on the façade is highly correlated to the albedo
 245 coefficient and to direct sun exposure. The higher surface temperature is reached by the C2 configuration, characterized

246 by high emissivity ($\epsilon = 0.96$) and low reflectivity ($\rho = 0.2$). In fact, as presented in Figure 5, black materials (lower albedo
247 coefficient) reach a surface temperature of around 55 °C while materials with high albedo (i.e., white color) show
248 temperature levels 15-20 °C lower.



249 a) b)
250 *Figure 5. Color effect on temperature comparison for the 45° orientation on June 21st. a) Average surface*
251 *temperatures daily trend. b) Surface temperatures inside the canyon (June 21st) for different materials*

252 Although the black material is the most critical, and such facades should be intervened promptly (unless mostly
253 shaded), grey was chosen for the canyon archetype since it is more representative of streets and buildings. In conclusion,
254 the canyon archetype selected for the green infrastructure mitigation potential analysis is characterized by a H/W equal
255 to 1, orientation 45° to the east, and a general albedo coefficient of the surfaces equal to 0.5.

256 3.2 UHI and AP mitigation measures impact analysis

257 All the measures have been simulated during the summer solstice for the time period between 1:00 pm to 8:00 pm;
258 to ensure model convergence before 2:00 pm (Most critical PET condition - Figure 5 a). However, the simulation results
259 have been displayed considering the values calculated at 2:00 pm, representing the most critical time period for both
260 temperatures and traffic pollution. In addition, at 2:00 pm, no shadows generated by the buildings could influence the
261 perceived temperature values.

262 3.2.1 UHI impact analysis

263 To study UHI, Figure 6 reports the perceived temperatures measured in PET for a middle cross-section of the
264 constructed archetype canyon, where different strategies have already been applied (G0-G7).

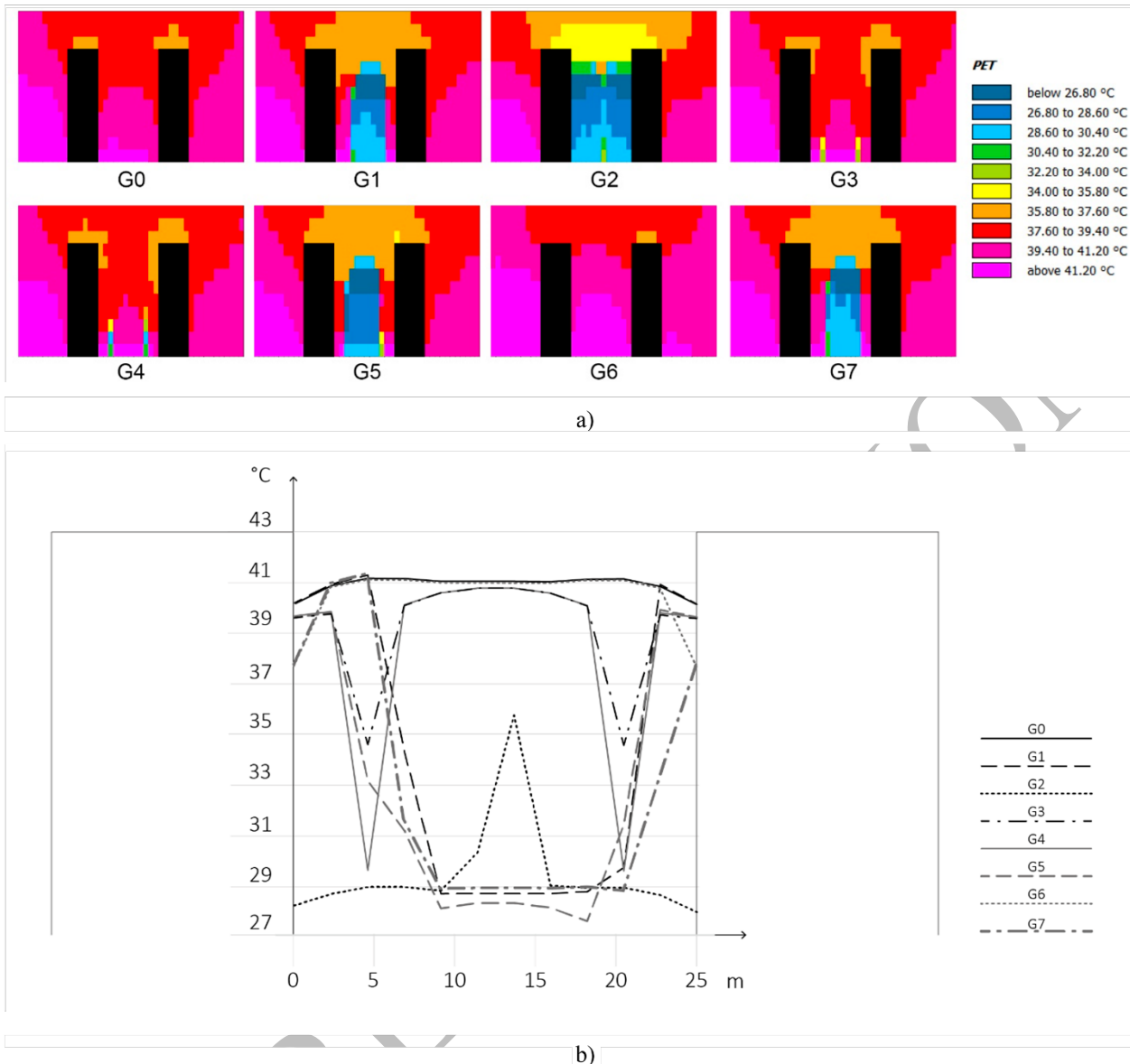


Figure 6. Simulation results of PET for all strategies inside the representative $H/W=1$ canyon at 2:00 pm on June 21st. a) Heat maps. b) Horizontal temperature at 1.5m height.

265

266

267

268

269

270

271

272

273

274

275

276

277

278

279

280

281

282

283

284

285

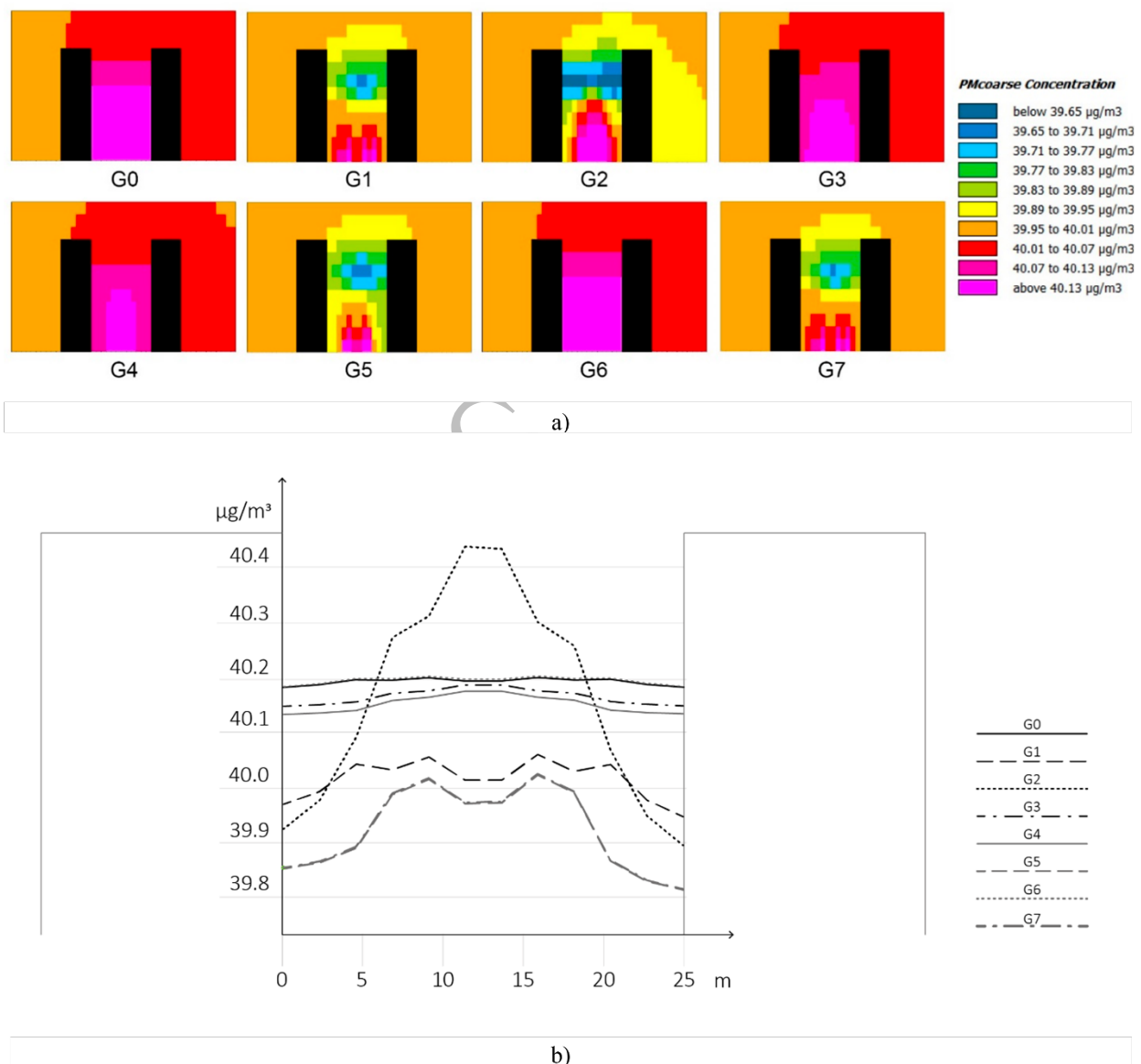
The perceived air temperature trend at a height of 1.5 m along the canyon section has been presented in Figure 6 b). The G0 configuration represents the base case where no vegetation is present in the canyon, used as a reference for comparing the different scenarios. In that case, the temperature level is homogenously high, with PET values close to 41 °C. The MS certainly led to different results; some have a clearly localized impact (e.g., G3 and G4) compared to others (G2, G5, G7). In fact, registered temperatures may vary from 27°C to 41 °C. For instance, looking at the values reported across the canyon section base, the results obtained for G1 simulation have a completely different trend compared to G0: on the edge of the street, temperatures are still around 40-41°C, but in the center, under the area of influence of the tree canopy, temperatures drop by more than 10°C potentially increasing the comfort level. Increasing the number of tree lanes and locating them closer to the canyon sidewalks (G2), the simulation results show a temperature level trend characterized by an extended lower and homogenous temperature area in proximity of the trees (28-29°C) with a punctual peak in the unshaded street center (35.7°C), evidently out of the area of influence of the trees. The temperature trends are different for the cases where the greenery is represented by hedges (1.5 m high for case G3 and 3m high for G4), having a very localized PET drop on the exact location where the hedges were placed. Probably given the low shading that these provide. The results show that in the area where hedges were applied, temperatures drop by 5°C for G3 and 10°C for G4 cases. The combined use of trees and hedges was studied in case G5. Such presence of multiple greenery leads to lower perceived temperatures with a minimum of 27.6°C found in the middle of the street, with a similar trend as G1, confirming a low spatial contribution of hedges against UHI. G6 and G7 cases combined the presence of 5 m high green walls, respectively, with and without a central row of trees. In general, as shown by the simulation results, the green wall (G6)

286 decreases the perceived temperature level on the sides of the canyon. In the G7 case, temperatures are lower than G6 due to
 287 to the presence of tree canopy that contributes to diminishing temperatures also in the central part of the canyon, thus
 288 confirming the considerable effect of high-level greenery MS, the low effect of low-level greenery MS and suggesting a
 289 negligible impact of green facades for pedestrians regarding UHI.

290
 291 *3.2.2 Air pollution impact analysis*

292 The same mitigation measures applied for lowering the UHI (G0-G7) are tested in terms of PM and NOx
 293 concentration. Both are screened given their high impact on human health, which can result in respiratory disease and/or
 294 cardio-circulatory system affections.

295 Figure 7 resumes the simulated PM concentrations in a middle section of the canyon. Such distribution follows the
 296 evidenced vortex generated by the north wind on an urban canyon with a 45° orientation, in which the pollutants
 297 dispersion is minimum in the middle upper part, where the primary vortex surges, and the leeward side. It is noteworthy
 298 to mention the small variations within the canyon, with an approximate amplitude of 0.48 µg/m³.



299
 300 *Figure 7. Simulation results of PM coarse concentration for all strategies inside the representative H/W=1 canyon*
 301 *at 2:00 pm on June 21st. a) Heat maps. b) Horizontal temperature at 1.5m height.*

302 As expected, different greenery configurations led to different PM concentration trends. The base case (G0) shows
 303 little variance in PM concentration in the contained air volume with values around 40.20 µg/m³. The configuration with
 304 one tree inside the street (G1) shows a moderate reduction of the PM concentrations throughout the section (vertical and

305 horizontal), with the minimum horizontal values on the street sides equal to $39.95 \mu\text{g}/\text{m}^3$, while the lowest values present
306 right above the tree canopy $39.65 \mu\text{g}/\text{m}^3$. In the configuration with two tree lanes (G2), the increased canopy density
307 seems to reduce the PM dispersion in the atmosphere under the tree canopy height while reducing PM concentrations
308 above it. The curve of MS G3 and G4 results show mutual similarity with the slightly reduced PM concentration on the
309 sides of the street, indicating that the hedges might act as barriers insufficiently protecting sidewalks from the more
310 polluted road. Nevertheless, the protection against road pollution is higher proportionally to the height of the greenery.
311 Case G5, representing the combined use of trees and hedges, shows the lowest pollutant concentration at the canyon's
312 sidewalks with levels between 39.8 and $40,0 \mu\text{g}/\text{m}^3$, which could be attributed to the air pollutant entrapment at street
313 level, generated by the low-level greenery acting as vertical barriers and the high-level greenery canopy acting as a
314 horizontal obstruction. For case G6 (green walls only), the PM concentration is similar to G0 because the PM moves
315 within the canyon before being deposited by the green wall. The case in which the green walls are applied together with
316 one row of trees (G7) shows a PM reduction similar to the G1 (single tree lane) and G5 configuration (hedges plus trees)
317 where even though there is a single row of trees, the correct ventilation of the canyon is not obstructed, and green barriers
318 absorb the pollutants underneath canopies. Therefore, it is possible to deduct that there is also a considerable effect of
319 high-level greenery MS, a localized and low effect of low-level greenery MS, and a negligible impact of green facades
320 for pedestrians regarding AP. Although, the integration of different types of vegetation (high and low-level greenery MS
321 – Trees plus hedges (G5)) is welcome and helps further increase the PM reduction for a more livable built environment
322 for pedestrians.

323 Figure 8 resumes the simulated NOx concentrations in a middle section of the canyon. Besides a significant variation
324 amplitude of approximately $16 \mu\text{g}/\text{m}^3$, the resulting air pollutant concentration follows the PM distribution trend.

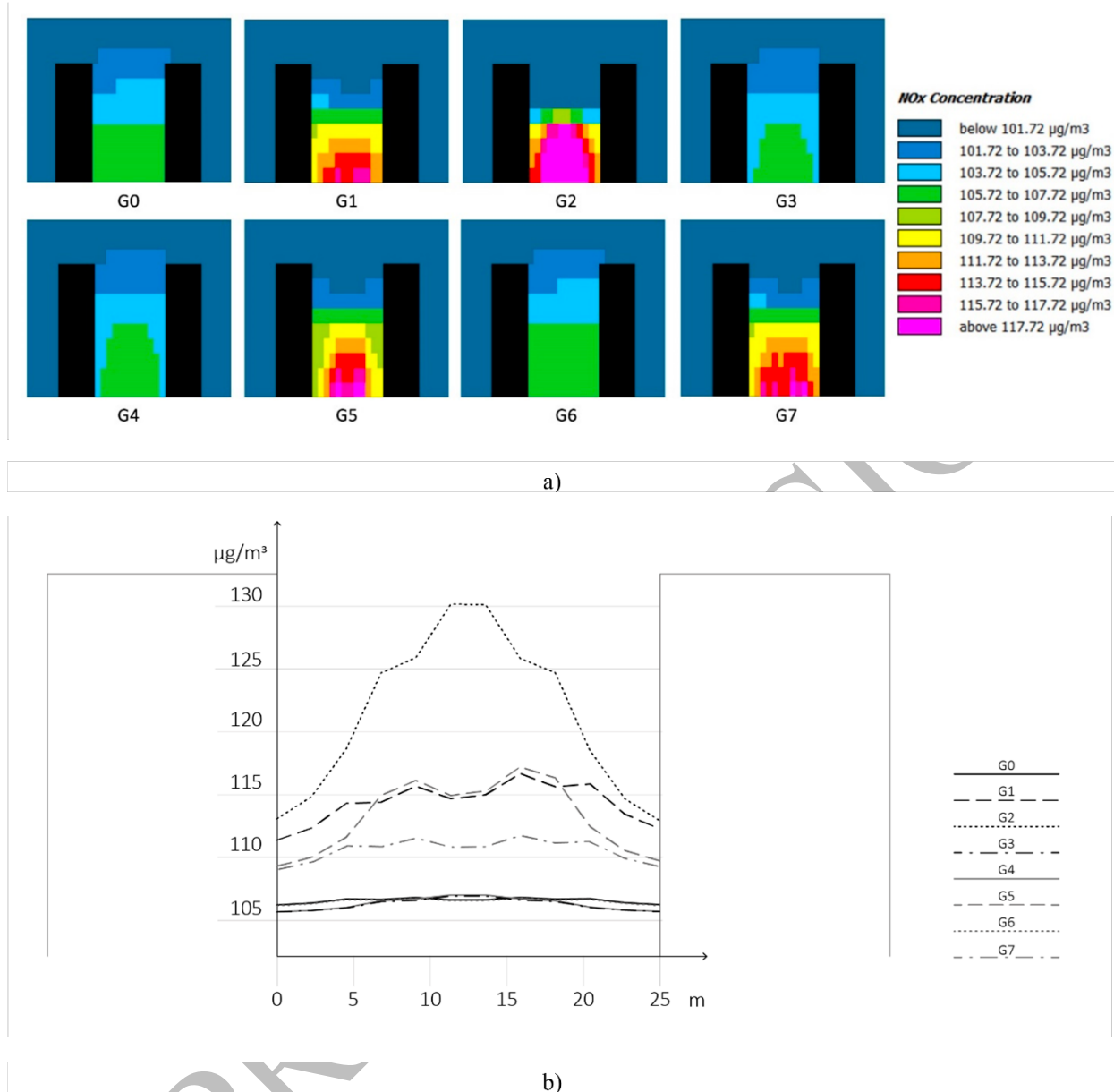


Figure 8. Simulation results of NOx concentration for all strategies inside the representative $H/W=1$ canyon at 2:00 pm on June 21st. a) Heat maps. b) Horizontal temperature at 1.5m height.

325

326

327

328

329

330

As experienced for PM coarse concentrations, not all greenery solutions act similarly. Compared to PM concentration, the scale of NOx concentrations is larger because traffic is more strongly linked with NOx emissions than PM.

331

332

333

334

335

336

337

338

All MS involving trees (G1, G2, G5, and G7) generally reach higher NOx concentrations. This is probably due to the presence of tree canopies that can obstruct the wind flow and thus the natural dissipation of the air pollutants emitted by traffic, resulting in air stagnation, hence the higher concentration of pollutants below naturally generated canopies. Meanwhile, G3 and G4 (low-level greenery MS) performed best, creating a barrier from traffic on the street towards the pedestrians on the sidewalks. Green facades (G6) showed no noticeable difference from the baseline scenario. This can be attributed to their low effect of them on wind flow dynamics and the low air pollutant deposition capacity of the selected species. Considering NOx only, high-level greenery MS has a rather detrimental effect than low-level greenery MS.

339

340

341

Aggregating PM and NOx results, the implementation of hedges will efficiently protect users on sidewalks from traffic emissions. At the same time, trees with low foliage density could also be used to guarantee correct canyon ventilation, facilitating NOx dispersion and PM protection.

342 4. Conclusions

343 The present study has been carried out to identify and quantify the potential UHI and AP mitigating effects of typical
344 greenery solutions applicable in urban canyons of dense BE. Through computer-aided simulation, the proposed method
345 has been proven useful and verified that natural-based solutions (i.e., vegetation) could positively impact both perceived
346 temperatures and air pollution concentration, but not in all cases as it is commonly expected. Some measures positively
347 impact mitigating the effect of both UHI and AP, while others mitigate only one of them. Therefore, because results
348 depend on many factors, interventions in the built environment shall be studied and tailored for the specific case, and it
349 is impossible to establish a unique optimal strategy for all cities and critical areas. Hence, identifying, utilizing, and
350 investigating a canyon archetype allows for standardizing the process and predicting the potential effects of vegetation
351 that must be considered progressively more in the urban design process. Despite there might be levels of uncertainty in
352 this analysis due to the considered scale, the results partially confirmed what has been stated in the literature. In general,
353 from the results of the H/W=1 urban canyon, the following considerations can be made:

- 354 - The use of trees is a promising option to tackle the UHI effect. The canopies can decrease the PET by 9-15°C and
355 benefit users' well-being.
- 356 - Green walls have, in general, a lower impact on PET reduction. The low albedo of the foliage can sometimes
357 increase the outdoor temperature level.
- 358 - The tree canopy can reduce airflow into the canyon, reducing pollutants dispersion. Proper tree distribution and
359 foliage density must be carefully considered.
- 360 - Considering NO_x, the integration of hedges represents a good strategy for containing traffic pollution in the road
361 section. From the perceived temperature point of view, the hedges are locally useful if they are sufficiently high.
362 A 3m hedge, with its shade, can diminish PET up to 6°C. However, a high hedge is a visible obstacle inside the
363 canyon that might not be visually appealing.
- 364 - Trees and hedges were proven to be valid options when dealing with UHI and AP.

365 Nevertheless, the results hereby presented are incomplete and could differ; thus, more research is foreseen to
366 complement them. For instance, the analysis was mainly performed on a single day with the highest solar angle, but it
367 might not be the hottest day. Also, the analysis carried out considering the contribution of wind was limited as a single
368 wind speed and direction was set.

369 5. Author Contributions

370 Conceptualization of the research, G.S. and E.Q.; conceptualization of the paper, G.S, J.D.B.C, and M.C.;
371 methodology, G.S, J.D.B.C, and M.C.; investigation, G.S, J.D.B.C.; data curation, M.C. and G.S.; writing - review and
372 editing, G.S, J.D.B.C, M.C., and E.Q.; data visualization M.C.; supervision, G.S.; project administration, G.S., and E.Q.;
373 funding acquisition, G.S., and E.Q. All authors have read and agreed to the published version of the manuscript.

374 6. Funding

375 This research was funded by the MIUR (the Italian Ministry of Education, University, and Research) Project BE
376 S2ECURe - (make) Built Environment Safer in Slow and Emergency Conditions through behavioral assessed/designed
377 Resilient solutions (grant number: 2017LR75XK).

378 7. References

- 379 [1] U.S. Environmental Protection Agency (2008) Urban Heat Island Basics. In: Reducing Urban Heat Island:
380 Compendium of Strategies. Draft. <https://www.epa.gov/heatislands/heat-island-compendium>. Accessed June 14th
381 2022
- 382 [2] United Nations (2018) World Urbanization Prospects 2018. In: Department of Economic and Social Affairs. World
383 Population Prospects 2018. [https://www.un.org/development/desa/publications/2018-revision-of-world-
384 urbanization-prospects.html](https://www.un.org/development/desa/publications/2018-revision-of-world-urbanization-prospects.html). Accessed June 14th 2022
- 385 [3] Salvalai G, Quagliarini E, Blanco Cadena JD (2020) Built environment and human behaviour boosting Slow-onset
386 disaster risk. Paper presented at the 7th International Conference on Heritage and Sustainable Development, Green
387 Lines Institute for Sustainable Development, Coimbra, 8-10 July 2020
- 388 [4] Tiwari A, Kumar P (2020) Integrated dispersion-deposition modelling for air pollutant reduction via green
389 infrastructure at an urban scale. *Sci Total Environ* 723:138078. doi:10.1016/j.scitotenv.2020.138078
- 390 [5] Santamouris M (2007) Heat Island Research in Europe: The State of the Art. *Adv Build Energy Res* 1(1):123-150.
391 doi:10.1080/17512549.2007.9687272

- 392 [6] Rajé F, Tight M, Pope FD (2018) Traffic pollution: A search for solutions for a city like Nairobi. *Cities* 82:100-107.
393 doi:10.1016/j.cities.2018.05.008
- 394 [7] Blanco Cadena JD, Salvalai G, Quagliarini E (2023). Determining behavioural-based risk to SLODs of urban public
395 open spaces: Key performance indicators definition and application on established built environment typological
396 scenarios. *Sustainable Cities and Society*: 95,2023. doi:10.1016/j.scs.2023.104580
- 397 [8] Andreou E (2014) The effect of urban layout, street geometry and orientation on shading conditions in urban canyons
398 in the Mediterranean. *Renew Energ* 63:587-596. doi:10.1016/j.renene.2013.09.051
- 399 [9] Biaio L, Cunyan J, Lu W et al (2019) A parametric study of the effect of building layout on wind flow over an urban
400 area. *Build Environ* 160(8):106160. doi:10.1016/j.buildenv.2019.106160
- 401 [10] Erell E, Pearlmutter D, Boneh D et al (2014) Effect of high-albedo materials on pedestrian heat stress in urban street
402 canyons. *Urban Clim* 10(2):367-386. doi:10.1016/j.uclim.2013.10.005
- 403 [11] Xie N, Li H, Abdelhady A et al (2019) Laboratorial investigation on optical and thermal properties of cool pavement
404 nano-coatings for urban heat island mitigation. *Build Environ* 147:231-240. doi:10.1016/j.buildenv.2018.10.017
- 405 [12] EPA United States Environmental Protection Agency (2022) Using Cool Roofs to Reduce Heat Islands.
406 <https://www.epa.gov/heatislands/using-cool-roofs-reduce-heat-islands>. Accessed June 14th 2022
- 407 [13] Nazarian N, Dumas N, Kleissl J et al (2019) Effectiveness of cool walls on cooling load and urban temperature in a
408 tropical climate. *Energy Build* 187:144-162. doi:10.1016/j.enbuild.2019.01.022
- 409 [14] S. M. Zaid, E. Perisamy, H. Hussein, N. E. Myeda, and N. Zainon (2018) “Vertical Greenery System in urban tropical
410 climate and its carbon sequestration potential: A review,” *Ecol. Indic.* 91:57–70, doi: 10.1016/j.ecolind.2018.03.086.
- 411 [15] Hong W, Guo R, Tang H (2019) Potential assessment and implementation strategy for roof greening in highly
412 urbanized areas: A case study in Shenzhen, China. *Cities* 95:102468. doi:10.1016/j.cities.2019.102468
- 413 [16] Kleerekoper L, Van Esch M, Salcedo TB (2018) How to make a city climate-proof: Addressing the urban heat island
414 effect. In: Hamlin Infield EM, Abunnasr Y, Ryan RL (ed) *Planning for Climate Change: A Reader in Green
415 Infrastructure and Sustainable Design for resilient Cities*, 1st edn. Taylor and Francis, New York, p 250-262
- 416 [17] Gromke C, Ruck B (2007) Influence of trees on the dispersion of pollutants in an urban street canyon – Experimental
417 investigation of the flow and concentration field. *Atmos Environ* 41(16):3287-3302.
418 doi:10.1016/j.atmosenv.2006.12.043
- 419 [18] Janhäll S (2015) Review on urban vegetation and particle air pollution – Deposition and dispersion. *Atmos Environ*
420 105:130-137. doi:10.1016/j.atmosenv.2015.01.052
- 421 [19] Labdaoui K, Mazouz S, Reiter S et al (2021) Thermal perception in outdoor urban spaces under the Mediterranean
422 climate of Annaba, Algeria. *Urban Clim* 39:100970. doi:10.1016/j.uclim.2021.100970
- 423 [20] Letter C, Jäger G (2019) Simulating the potential of trees to reduce particulate matter pollution in urban areas
424 throughout the year. *Environ Dev Sustain* 22:4311-4321 (2020). doi:10.1007/s10668-019-00385-6
- 425 [21] Salim SM, Buccolieri R, Chan A et al (2009) Urban Air Quality Management: Effect of Trees on Air Pollution
426 Concentrations in Urban Street Canyons. Paper presented at the U21 Graduate Research Conference: Sustainable
427 Cities for the Future, Venue Universities of Melbourne & Queensland (Brisbane), Australia, 29 November-05
428 December 2009
- 429 [22] Van Ryswyk K, Prince N, Ahmed M et al (2019) Does urban vegetation reduce temperature and air pollution
430 concentrations? Findings from an environmental monitoring study of the Central Experimental Farm in Ottawa,
431 Canada. *Atmos Environ* 218:116886. doi:10.1016/j.atmosenv.2019.116886
- 432 [23] Synnefa A, Dandou A, Santamouris M et al (2008) On the Use of Cool Materials as a Heat Island Mitigation Strategy.
433 *J Climatol Appl Meteorol* 47(11):2846-2856. doi:10.1175/2008JAMC1830.1
- 434 [24] Abdo P, Phuoc Huynh B (2021) An experimental investigation of green wall bio-filter towards air temperature and
435 humidity variation. *J Build Eng* 39:102244. doi:10.1016/j.jobe.2021.102244
- 436 [25] Berardi U, GhaffarianHoseini AH, GhaffarianHoseini A (2014) State-of-the-art analysis of the environmental
437 benefits of green roofs. *Appl Energy* 115:411-428. doi:10.1016/j.apenergy.2013.10.047
- 438 [26] Speak AF, Rothwell JJ, Lindley SJ et al (2012) Urban particulate pollution reduction by four species of green roof
439 vegetation in a UK city. *Atmos Environ* 61:283-293. doi:10.1016/j.atmosenv.2012.07.043

- 440 [27] British Standard Institution (BSI), "BS 8206-2 - Lighting for buildings – Part 2: code of practice for daylighting,"
441 B.S. Inst., 2008.
- 442 [28] S. A. Salleh, Z. A. Latif, B. Pradhan, W. M. N. Wan Mohd, and A. Chan (2014) "Functional relation of land surface
443 albedo with climatological variables: a review on remote sensing techniques and recent research developments,"
444 Geocarto Int. 29:147–163, doi: 10.1080/10106049.2012.748831
- 445 [29] Höppe P (1999) The physiological equivalent temperature – a universal index for the biometeorological assessment
446 of the thermal environment. Int J Biometeorol 43:71-75. doi:10.1007/s004840050118
- 447 [30] ISO. (2004). EN ISO 8996: Ergonomics of the thermal environment - determination of metabolic rate. Geneva:
448 International Standardisation Organisation, 3.

IN-PRESS VERSION